Approximate Solution for a Nonisothermal Gas Bubble Growth over a Spherical Heating Element

M. Kostoglou* and T. D. Karapantsios

Division of Chemical Technology, Department of Chemistry, Aristotle University, University Box 116, 541 24 Thessaloniki, Greece

Recent experimental evidence has shown that single bubble generation on miniature heating elements is a competitive alternative to massive bulk bubble generation for the study of gas/vapor bubble growth dynamics. The inherent two-dimensionality of the problem leads to significant deviations of the bubble growth with respect to the bulk bubble growth which can be approximated by the classical one-dimensional (spherically symmetric) theory. In the present work, an approximate theory is developed, valid for a certain region of the problem parameters, which permits computation of the bubble radius evolution curves. On the basis of these results, the effect of the two-dimensionality (axial symmetry) of the problem on the bubble growth characteristics is assessed. The approximate solution developed here is of particular interest, since the complete solution using computational fluid dynamics (CFD) techniques is not practically feasible at this moment because of the large number of size and time scales involved in the problem.

1. Introduction

The generation and growth of bubbles in liquids containing dissolved gases—because of supersaturation degassing—is a very important process in diverse scientific fields. Some of these are as follows: materials technology, e.g., plastic foam manufacturing;[1,2] human physiology, e.g., blood oxygenation, bubbles growing in the tissue of humans (divers, astronauts, and high altitude airplane passengers, during decompression incidents);[3−5] geology, e.g., volcanic eruptions due to magma degassing;[6,7] food technology;[8] and environmental applications, e.g., wastewater treatment by dissolved air flotation.[9,10] The degassing process shares many common features with the boiling process (vapor bubble generation)[11] but also has prominent differences, with the most important being the enormously different size and time scales involved in the two processes.

In the traditional experimental studies dealing with degassing liquids, the visual observation of an isolated growing bubble is a difficult task, because bubbles are generated in large numbers in the bulk of the liquid by applying a sudden global decompression. Visual observation is hindered further by the fact that decompression is usually implemented by a volume change which induces convective currents in the liquid that cause the developing bubbles to drift away from their nucleation sites. To overcome this problem, an experimental design has been proposed[12] which permits the generation of just a single bubble in the liquid. This is realized by using a miniature spherical thermistor as a heater, submerged in the bulk of the liquid. The thermistor is suddenly heated, and as the liquid becomes locally supersaturated with respect to the dissolved gas, a bubble forms at the surface of the thermistor. Subsequently, the bubble grows with the transfer of mass of the dissolved gas from the bulk of the liquid to the bubble surface. An experimental campaign was performed under microgravity conditions (necessary for eliminating the effects of bubble buoyancy and natural convection) in order to obtain results amenable to rigorous theoretical interpretation.

An initial attempt to simulate the problem of bubble growth on the thermistor was based on a spherically symmetric (1-D) model of a spherical bubble growing at a uniform temperature (equal to the thermistor temperature) and a far field temperature equal to the initial bulk liquid temperature. The problem was solved using a well-known similarity transformation[13,14] and has led to a power law relation between bubble radius and time with an exponent value equal to 0.5. However, the corresponding experimental curves were best-fitted by lower (than 0.5) exponent values. According to the model, this meant that the bubble temperature should decrease with time. Part of this temperature decrease was attributed to the small temperature decrease of the thermistor during heating, which, however, was not enough to match the predicted low bubble temperature. Another weak point of the above view of the process is that the computed power needed to sustain the bubble growth in the cold fluid (mainly to compensate conductive losses from the bubble's surface) was larger than the actual power delivered by thermistor.

To have a more realistic perspective, the two-dimensional (axial symmetric) character of the problem must be taken into account. The bubble initially grows not in a cold fluid (as it was assumed) but inside the temperature field developing around the thermistor. In that case, the bubble temperature may decrease not because of the thermistor temperature decrease (measured to be small anyway) but because it is exposed to a gradually colder fluid as it grows. Apparently, this new perspective of the problem presupposes a two-dimensional (2-D) temperature distribution inside the bubble instead of a constant bubble temperature. In the present work, the 2-D aspects of the problem are examined in

* Corresponding author. Tel.: +30 2310 99 7767. Fax: +30 2310 99 7759. E-mail: kostoglu@chem.auth.gr.

10.1021/ie050600c CCC: $30.25
Published on Web 09/13/2005

order to appraise their influence on the bubble radius evolution curves.

To this end, an approximate solution for the problem of a gas bubble growing in contact with a spherical thermistor is derived at the limit of fast heat transfer and slow mass transfer in the liquid with respect to bubble growth dynamics (a case relevant to practical situations). In the analysis, the effect of thermocapillary motion is ignored (a zero Marangoni number for both heat and mass transfer is assumed). Nevertheless, this effect is well-appreciated, so its influence on bubble growth is discussed extensively. The present problem has some relevance to the problem of subcooled nucleate boiling,[15,16] where there is also a temperature distribution along the bubble surface (depending on the Marangoni number) which determines the local mass transfer (evaporation−condensation rate). Yet, one must keep in mind that the bubble-growth time scale in the present problem is about 10^4 times slower than that in the nucleate boiling problem.

The structure of the present work is the following: At first, the mathematical problem describing the bubble growth on a heated thermistor is presented together with the necessary assumptions based on the actual physics of the problem. The additional assumptions required for the derivation of the approximate solution are also listed. In the next section, the approximate solution of the bubble growth problem is derived step by step. Finally, some general results and some for the particular system CO_2−water are presented and discussed in a comprehensive manner.

2. Problem Formulation

On the basis of the experimental observation of the very small (nearly zero) contact angle of the liquid on the thermistor's surface (glass), the bubble is assumed to have the shape of a sphere having a point contact with the thermistor. The complete physical problem is very complicated and includes the following: (a) transient heat conduction equation with a nonlinear heat source (temperature-dependent ohmic resistance) in the thermistor; (b) Navier−Stokes equation in the fluid (liquid and bubble) domains [the liquid motion is set by (i) the bubble growth and (ii) the thermocapillary motion due to a temperature gradient on the bubble surface]; and (c) transient convection−diffusion equation for heat and mass transfer in the two fluid domains.

Several simplifications can be made based either on the physics of the problem or on geometrical considerations in order to define the model problem for which the descriptive equations can be solved at a reasonable effort. These simplifications are as follows:

(1) The thermistor is assumed to be spherical, having a constant temperature T_e due to the large ratio of the thermistor's material thermal diffusivity to the liquid thermal diffusivity.

(2) Thermal and mass diffusivity are two orders of magnitude larger in the bubble gas than in the surrounding liquid, so transient and convection effects can be ignored inside the bubble while this is not possible for the liquid phase.

(3) All transport properties are assumed to be constant (independent from temperature).

(4) The density and thermal conductivity of the bubble gas is negligibly small in comparison with those of the liquid.

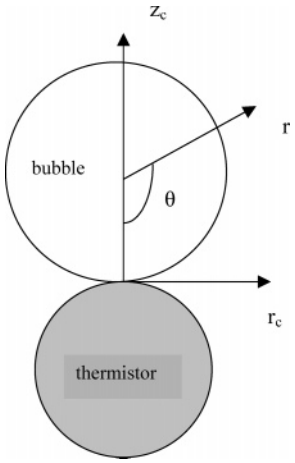

Figure 1. Schematic of the problem. The spherical-coordinate system (r,θ) and the cylindrical coordinate system (r_c, z_c) are also shown.

(5) The evaporation of liquid on the bubble−liquid interface occurs infinitely fast. This means that thermodynamic equilibrium is assumed at the interface, with the assumption of an ideal mixture, so that the mole fraction of the vapor at the interface can be directly related to the instantaneous temperature, and the solute gas concentration in the liquid at every point on the interface is the equilibrium solubility corresponding to the temperature at that point. This leads to variation of the gas phase mole fraction along the interface, which is a significant difference from the spherically symmetric model. In addition, the latent heat of the evaporating liquid can be shown to be insignificant with respect to the heat flux from the thermistor, so it can be ignored.

(6) The bubble growth is very slow with respect to flow dynamics, so a pseudo-steady-state flow field can be assumed.

(7) The growth rate is very slow with respect to heat transfer dynamics in the liquid, so a pseudo-steady-state temperature profile can be assumed. This is the most essential assumption up to now. For the system water−CO_2 examined by Divinis et al.,[12] the characteristic heat transfer time is 0.1 s for the system thermistor−water and even smaller for the bubble−water system; it is clear that, for the growth rates observed in the experiments, the pseudo-steady-state assumption is valid. The above condition may be violated at very small times when the bubble grows very fast, but this is not really a problem since, initially (at small bubble sizes), the bubble temperature is almost constant and heat transfer is not critical. The geometry of the problem and the definition of two of the coordinate systems used here are shown in Figure 1. Given the above assumptions, the problem is described in mathematical terms as follows.

Field Equations.

Bubble domain:

$$\nabla^2 T_g = 0 \tag{1}$$

$$\nabla^2 x_v = 0 \tag{2}$$

where T_g is the gas temperature and x_v is the vapor molar fraction in the bubble.

Liquid domain:

heat conservation (pseudo-steady-state)

$$\rho_l C_p \vec{u}\vec{\nabla}T = k\nabla^2 T \quad (3)$$

gas mass conservation (transient)

$$\frac{\partial c}{\partial t} + \vec{u}\vec{\nabla}c = D\nabla^2 c \quad (4)$$

continuity equation $\vec{\nabla}\vec{u} = 0$ (5)

Navier−Stokes (pseudo-steady-state) $\vec{u}\vec{\nabla}\vec{u} = \nu\nabla^2\vec{u}$ (6)

where T is the liquid temperature, c is the dissolved gas concentration in the liquid, and $\vec{u}$ is the velocity field in the liquid. The symbols k, υ, and D denote the liquid thermal conductivity, the liquid kinematic viscosity, and the gas-in-liquid diffusion coefficient, respectively. The density ρ_l and the specific heat capacity C_p refer to the liquid phase.

Boundary Conditions.

At S_1 (thermistor's surface):

constant thermistor's temperature $T = T_e$ (7a)

No-slip condition for liquid velocity $\vec{u} = 0$ (7b)

No-gas-penetration condition $\frac{\partial c}{\partial \vec{n}} = 0$ (7c)

where $\vec{n}$ denotes the direction normal to the surface.

At S_2 (bubble surface), liquid side:

$$c = c_{eq}(T) \quad (8a)$$

where c_{eq} is the solubility of gas in the liquid at temperature T.

No heat penetration towards the bubble $\frac{\partial T}{\partial \vec{n}} = 0$ (8b)

This condition emerges from the small value of the gas-to-liquid thermal conductivities ratio.

The normal velocity of the liquid on the surface of a bubble which grows while keeping constant not its center but a particular point of its surface (contact point with the thermistor) is

$$u_n = \frac{dR}{dt}(1 + \cos\theta) \quad (8c)$$

where θ is the angular coordinate of a system of spherical coordinates r, θ (no φ dependence is considered due to axis symmetry) having as its center the center of the bubble. The point $r = R$, $\theta = 0$ corresponds to the bubble−thermistor contact point.

The appearance of shear stress on the surface of the bubble due to the surface distribution of surface tension γ is induced by the surface distribution of temperature. This boundary condition is responsible for the onset of thermocapillary motion in the liquid.

$$\tau_{ns} = \frac{1}{R}\frac{d\gamma}{d\theta} \quad (8d)$$

where s is the local tangential to the interface coordinate.

The local vapor molar fraction at the surface of the bubble can be found from the vapor pressure of the liquid P_L and the total pressure P_t.

At S_2 (bubble surface), gas side:

$$x_v = \frac{P_L(T)}{P_t} \quad (9a)$$

At the gas/liquid interface, the two temperatures must be the same.

$$T_g = T \quad (9b)$$

Far-Field Conditions. For a large enough experimental cell, one can assume an infinite medium with far-field temperature and concentration equal to the initial ones (corresponding to saturation conditions).

$$T = T_o \quad (10a)$$

$$c = c_o = c_{eq}(T_o) \quad (10b)$$

Total Mass Balance Condition. The global gas balance determines the bubble growth rate as follows,

$$\frac{4\pi}{3}\frac{d\rho_{gave}R^3}{dt} = D\int_{S_2}\frac{\partial c}{\partial \vec{n}}\,dS \quad (11)$$

where the average gas molar density in the bubble can be found from

$$\rho_{gave} = \frac{1}{V_b}\int_{V_b}(1 - x_v)\frac{P_t}{R_g T_g}\,dV \quad (12)$$

The equations for the surfaces S_1 and S_2 in the cylindrical coordinate system (r_c, z_c), having as its origin the contact point between bubble and thermistor, are as follows:

thermistor:

$$(z_c + R_h)^2 + r_c^2 = R_h^2 \quad (13)$$

bubble:

$$(z_c - R)^2 + r_c^2 = R^2 \quad (14)$$

where R_h denotes the radius of the thermistor.

The initial conditions for the above problem are that, at time $t = 0$ (moment of nucleation), the bubble radius is $R = 0$ and the concentration everywhere is $c = c_o$. It is implicitly assumed in the above formulation that the temperature profile around the thermistor is already developed at $t = 0$, so an initial temperature condition is not needed.

The above mathematical problem is extremely difficult to be solved, since it contains an evolving interface

in two dimensions combined with the solution of Navier–Stokes and convection–diffusion equations in moving domains. The following limiting case will be considered here in order to examine the effect of the particular two-dimensional geometry on the bubble growth rate, avoiding the solution for the flow field.

(i) At first, the thermocapillary flow around the bubble is ignored (both thermal and mass Marangoni number are assumed zero). Usually, this is not the case under realistic conditions, but the effect of thermocapillarity is so clear that omitting practically means that the present solution can assess the upper limit of the effect of geometry on bubble growth. Thermocapillary flow carries water from the bubble base (thermistor) to the bubble apex, thus reducing the temperature difference along the bubble surface. In other words, thermocapillarity opposes the two-dimensionality effect, which would tend to decrease the bubble temperature.

(ii) The limit of fast growth with respect to diffusion is considered. This means that the dissolved species have no time to diffuse as the bubble grows, so the concentration gradient is restricted to a very thin layer around the bubble. The limit of a growth rate that is slow with respect to heat transfer and fast with respect to mass transfer is realistic since, in general, mass transfer in liquids is slower than heat transfer.

3. Problem Solution

3.1. Pseudo-Steady-State Heat Transfer in Liquid. In the absence of a velocity field, the Laplace equation with boundary conditions from eqs 7a and 8b must be solved for the temperature distribution in the liquid. All the spatial coordinates in this subsection are nondimensionalized with respect to the thermistor radius, R_h, and the temperature is nondimensionalized as $\bar{T} = (T - T_o)/(T_e - T_o)$. To use the separation-of-variables technique for the solution of the Laplace equation in bispherical-coordinates, the more general problem of two spheres with arbitrary separation distance will be considered. The bispherical system of coordinates ξ, μ ($-\infty < \xi < \infty$, $-1 < \mu < 1$) is defined as follows:

$$r_c = \frac{\sinh \alpha \sqrt{1-\mu^2}}{\cosh\xi - \mu} \tag{15}$$

$$z = \frac{\sinh \alpha \sinh \xi}{\cosh \xi - \mu} \tag{16}$$

In this system, the surfaces of the thermistor and the bubble are defined by $\xi = \alpha$ ($\alpha > 0$) and $\xi = \beta$ ($\beta < 0$), respectively. The new cylindrical system (r_c, z) has its z-axis origin at a distance cosh α from the center of the thermistor toward the bubble. If the ratio of the bubble radius to the thermistor radius is q and their dimensionless minimum distance (distance between closest points) is h, the values α, β can be found from the solution of the following system of equations:

$$q = \frac{-\sinh \alpha}{\sinh \beta} \tag{17}$$

$$h = \cosh \alpha + q \cosh \beta - q - 1 \tag{18}$$

The general solution of the Laplace equation for the particular coordinate system is[17]

$$\bar{T} = (\cosh \xi - \mu)^{1/2} \sum_{i=0}^{\infty} (a_i \cosh((i + 1/2)\xi) + b_i \sinh((i + 1/2)\xi) P_i(\mu) \tag{19}$$

where P_i are the Legendre polynomials and a_i and b_i are constants which must be determined from the boundary conditions. By requiring $\bar{T} = 1$ on the thermistor's surface ($\xi = \alpha$) and employing the orthogonality properties of Legendre polynomials, the coefficients b_i can be eliminated leading to

$$\bar{T} = (\cosh \xi - \mu)^{1/2} \sum_{i=0}^{\infty} (a_i F_i(\xi) + H_i(\xi)) P_i(\mu) \tag{20}$$

where

$$F_i(\xi) = \cosh((i + 1/2)\xi) - \frac{\sinh((i + 1/2)\xi)}{\tanh((i + 1/2)\alpha)} \tag{20a}$$

$$H_i(\xi) = (i + 1/2)\sqrt{2} e^{-(i+1/2)|\alpha|} \frac{\sinh((i + 1/2)\xi)}{\sinh((i + 1/2)\alpha)} \tag{20b}$$

Requiring a zero normal derivative of the temperature field (eq 20) on the bubble's surface ($\xi = \beta$) and employing the relation $\mu P_i = (i/(2i + 1))P_{i-1} + ((i + 1)/(2i + 1))P_{i+1}$ leads to the following infinite system of equations for the a_i's ($i = 0, 1, 2, ..., \infty$),

$$\left((\cosh \beta)F_i'(\beta) + \frac{1}{2}(\sinh \beta)F_i(\beta)\right)a_i - \frac{i+1}{2i+3}F_{i+1}'(\beta)a_{i+1} - \frac{i}{2i-1}F_{i-1}'(\beta)a_{i-1} = -(\cosh \beta)H_i'(\beta) - \frac{1}{2}(\sinh \beta)G_i(\beta) + \frac{i+1}{2i+3}H_{i+1}'(\beta) + \frac{i}{2i-1}H_{i-1}'(\beta) \tag{21}$$

where the prime denotes differentiation of the function with respect to its argument.

To proceed, the above system must be truncated to a value $i = n$. The coefficient a_{n+1} is met in the last equation, so the system is not closed (more unknowns than equations). The usual approach is that, if n is adequately large, the value of a_{n+1} is negligibly small, so it can be set equal to zero.[18] It is found here that, although this works perfectly for $q < 1$, the procedure becomes unstable for $q > 1$. In that case, the finite value of a_{n+1} is always needed for the solution of the system in eq 21, regardless of how small it is. To overcome this problem, an asymptotic analysis of eq 21 in the limit $i \to \infty$ was performed, and it led to $a_i \to \sqrt{2} e^{(2i+1)\alpha}$ as $i \to \infty$. This relation can be used for the estimation of a_{n+1} for appropriately large n in the system in eq 21. Another problem is that the number of terms n needed for convergence increases as h becomes smaller, and the problem becomes singular in the case of spheres in contact ($h = 0$). This is not due to a real singularity of the temperature field but to the inability of the bispherical-coordinate system to describe the touching spheres geometry. All the computations will be performed here for $h = 0.01$, which gives practically the same result as the case $h = 0$. The number of terms needed for convergence are from $n = 60$ to $n = 120$. The

spherical system of coordinates (r, θ) associated with the bubble is needed for intrabubble calculations and for presenting the surface temperature distribution. The relation between the bispherical coordinate μ and the spherical coordinate θ on the bubble's surface is

$$\mu = \cosh(\beta) - \frac{\sinh^2(\beta)}{\cosh\beta - \cos\theta} \tag{22}$$

This relation is used to get the bubble surface temperature distribution in terms of θ, required for the analysis of the intrabubble temperature distribution.

3.2. Intrabubble Heat and Mass Transfer. The gas temperature and the vapor molar fraction distributions must be known in order to compute the mean gas density ρ_{gave}. Having found the temperature along the bubble surface as a function of angle θ (let us say $T_s(\theta)$), the corresponding vapor molar fraction distribution ($x_{vs}(\theta)$) can be directly estimated using eq 9a. Both surface distributions must be used as boundary conditions for the solution of the corresponding Laplace eqs 1 and 2 in the bubble. The intrabubble temperature and vapor molar fraction fields can be found as

$$T_g(r,\theta) = \sum_{i=0}^{\infty} c_i r^i P_i(\cos\theta) \tag{23}$$

$$x_v(r,\theta) = \sum_{i=0}^{\infty} d_i r^i P_i(\cos\theta) \tag{24}$$

where the expansion coefficients c_i and d_i can be computed from

$$c_i = \frac{2i+1}{2}\int_0^{\pi} T_s(\theta) P_i(\cos\theta)\sin\theta\, d\theta \tag{25}$$

$$d_i = \frac{2i+1}{2}\int_0^{\pi} x_{vs}(\theta) P_i(\cos\theta)\sin\theta\, d\theta \tag{26}$$

Equations 23 and 24 must be replaced in the double integral for the average dissolved gas density. Numerical integration of the integrals in eqs 25 and 26—as for the double integral (over r, θ) in eq 11—is required, making the computation of ρ_{gave} cumbersome. Alternatively, taking into account the fact that the density variation in the bubble is expected to be small, the following approximation can be used:

$$\rho_{gave} = \frac{1}{V_b}\int_{V_b}(1 - x_v)\frac{P_b}{R_g T_g}\, dV \approx (1 - x_{vave})\frac{P_b}{R T_{gave}} \tag{27}$$

Integrating the expressions in eqs 23 and 24 over the bubble volume, all the modes disappear except from the zero-order mode, leaving the volume average equal to the surface average and making the computations of x_{vave} and T_{ave} trivial:

$$T_{ave} = \frac{1}{V_b}\int_{V_b} T\, dV = \frac{1}{2}\int_0^{\pi} T_s(\theta)\sin\theta\, d\theta \tag{28}$$

$$x_{vave} = \frac{1}{V_b}\int_{V_b} x_v\, dV = \frac{1}{2}\int_0^{\pi} x_{vs}(\theta)\sin\theta\, d\theta \tag{29}$$

3.3. Mass Transfer in Liquid. The assumption of a thin concentration boundary layer around the bubble's surface does not directly simplify the problem. Yet, if only the bubble growth history and not the exact concentration field in the liquid is of interest, the following approximations can be employed:

(i) The bubble evolution does not depend on the geometry. It has been shown that a bubble grows in contact with a solid wall exactly in the same manner as it grows in an infinite fluid.[19]

(ii) The mass transfer rate is proportional to the radial liquid velocity on the surface. This results from the expression for the bubble radius evolution in the limit of the thin concentration boundary layer.[13,14]

On the basis of the above, it can be assumed that the local mass transfer toward the bubble depends only on the local driving force ($c_o - c_{eq}$) and the local interface velocity in the normal direction.

The transient convection−diffusion equation for the concentration field during growth in an infinite liquid is solved for each point of the surface of the bubble, and then the interfacial flux is locally corrected for the radial velocity of the liquid at the interface. This technique gives the correct result for the growth rate of the isothermal case and, at the same time, accounts for the radial velocity distribution on the bubble's surface to properly weight the variation of flux induced by the temperature distribution. The approximate equation for the concentration field around the bubble in the spherical-coordinate system is as follows:

$$\frac{\partial c}{\partial t} + \frac{1}{r^2}\frac{dR}{dt}\frac{\partial c}{\partial r} = D\frac{\partial^2 c}{\partial r^2} \tag{30}$$

$$\text{at } r = R, \quad c = c_{eq}(T_s(\theta)) = c_s(\theta,R) \tag{31a}$$

$$\text{at } r = \infty, \quad c = c_o \tag{31b}$$

There is no explicit θ dependence in eq 30. The θ dependence of the concentration field is due exclusively to the boundary condition. This boundary condition also has a time dependency through the time dependency of R. Employing the following coordinate transformation,[20]

$$y = \frac{1}{3}(r^3 - R^3) \tag{32a}$$

$$g = D\int_0^t R^4(\tau)\, d\tau \tag{32b}$$

eq 30 takes the form

$$\frac{\partial c}{\partial g} = \frac{\partial^2 c}{\partial y^2} \tag{33}$$

The solution of this equation with boundary conditions eqs 31a and b is given by Ozisik[21] as

$$c(y,\theta,g) = c_o + \frac{y}{2\sqrt{\pi}}\int_{g'=0}^{g}(c_s(\theta,R) - c_o)\frac{e^{-y^2/(4(g-g'))}}{(g-g')^{3/2}}\, dg' \tag{34}$$

This form of solution is not well-suited for computations, since at $y = 0$ it becomes undefined, so it must be handled with asymptotic means to make computations for small values of y. The situation is even more difficult for the computation of the required derivative $(\partial c/\partial r)_{r=R}$. To overcome this problem, integration by parts is

performed to the integral of eq 34 to give the following convenient relation:

$$c(y,\theta,g) = c_o + \frac{2}{\sqrt{\pi}}(c_e - c_o)\int_{\xi=y/(2\sqrt{g})}^{\infty} e^{-\xi^2}\,d\xi + \frac{2}{\sqrt{\pi}}\int_{g'=0}^{g}\frac{\partial c_s(\theta,R)}{\partial g'}\int_{\xi=y/(2\sqrt{g-g'})}^{\infty} e^{-\xi^2}\,d\xi\,dg' \quad (35)$$

The concentration derivative on the bubble's surface can be computed from the above concentration field as follows:

$$\left(\frac{\partial c}{\partial r}\right)_{r=R} = R^2\left(\frac{\partial c}{\partial y}\right)_{y=0} = -R^2\frac{1}{\sqrt{\pi}}\left(\frac{c_e - c_o}{\sqrt{g}} + \int_{g'=0}^{g}\frac{\partial c_s(\theta,R)}{\partial g'}\frac{1}{\sqrt{g-g'}}\,dg'\right) \quad (36)$$

Substituting it into the gas mass balance equations leads to

$$\frac{4\pi}{3}\frac{d\rho_{gave}R^3}{dt} = -4\pi DR^4\frac{1}{\sqrt{\pi}}\int_{\theta=0}^{\pi}\left(\frac{c_e - c_o}{\sqrt{g}} + \int_{g'=0}^{g}\frac{\partial c_s(\theta,R)}{\partial g'}\frac{1}{\sqrt{g-g'}}\,dg'\right)\frac{(1-\cos\theta)\sin\theta}{2}\,d\theta \quad (37)$$

where the term $(1 - \cos\theta)$ has been added in order to correct the local gas flux to the bubble proportionaly with the local radial fluid velocity. The variation of the gas density is, in general, very small with respect to the variation of R^3, which varies by many orders of magnitude, so it can be placed out of the time derivative. The order of integration with respect to θ and g' can be interchanged. Finally, by denoting as ρ_e the gas density in temperature T_e and defining the dimensional gas density as $\bar{\rho}_{gave} = \rho_{gave}/\rho_e$, eq 37 can be written as follows,

$$\frac{dR}{dt} = DR^2F_m\frac{1}{\bar{\rho}_{gave}\sqrt{\pi}}\frac{1}{\sqrt{g}}\left(1 + \int_{g'=0}^{g}\frac{\partial\Phi(R)}{\partial g'}\frac{\sqrt{g}}{\sqrt{g-g'}}\,dg'\right) \quad (38)$$

where the foaming number, F_m, is defined for a bubble growing at a constant temperature T_e:

$$F_m = \frac{c_o - c_{eq}(T_e)}{\rho_e} \quad (39)$$

The function $\Phi(R)$ can be computed from the solution of the heat transfer problem as follows:

$$\Phi(R) = \int_0^{\pi}\left(\frac{c_s(\theta,R) - c_o}{c_e - c_o}\right)\frac{(1-\cos\theta)\sin\theta}{2}\,d\theta \quad (40)$$

Equation 38 must be solved simultaneously with

$$\frac{dg}{dt} = DR^4 \quad (41)$$

and initial conditions $R(0) = g(0) = 0$ to give the bubble radius evolution. The effect of two-dimensionality is included in the integral term of eq 38 and in $\bar{\rho}_{gave}$. If this integral term is omitted and $\bar{\rho}_{gave} = 1$, the constant temperature (spherically symmetric) bubble growth problem is recovered and the system of equations can be solved analytically to give $R = 2F_m\sqrt{(3/\pi)t}$, i.e., self-similar bubble growth in the limit of large Foaming number (thin concentration boundary layer).

Summarizing, let us assume that, at a particular time instant, the bubble radius is R. The temperature profile at this instant can be found by solving the system in eq 21 with $q = R/R_h$ and replacing a_i's in eq 20. From eqs 28, 20, and 22, the mean temperature in the bubble T_{ave} can be found. From eqs 29, 9a, 20, and 22, the mean vapor fraction in the bubble is computed. The concentration profile is given by eq 35, where g is a time-like variable given by eq 32b. Obviously, the complete history $R(t)$ must be available at each time instant. The function Φ is computed from eqs 40, 8a, 20, 22. Finally, the evolution of the bubble radius is given by eq 38.

3.4. Numerical Integration. The integrodifferential system of equations must be solved numerically. This is not a trivial task because of the stiffness of the differential system combined with the weak singularity in the integral in eq 38. This singularity must be removed by employing finite-analytic integration. Also, the stiffness of the differential system can be reduced by using a new independent variable $Z = R^2$. Any attempt to integrate the system using a constant time step fails. ODE's integrators cannot be used directly because of the existence of the integral in eq 38, but they can be used through consecutive calls in time intervals during which the derivative in the integral is assumed to have a constant value so analytical integration is possible. Surprisingly enough, even attempts of this type using a Runge−Kutta explicit integrator[22] failed. Finally, the following procedure led to success in numerically solving the system of equations (eqs 38 and 39):

(i) nondimensionalization:

$$\tau = \frac{Dt}{{R_h}^2},\quad \bar{R} = \frac{R}{R_h},\quad \bar{g} = \frac{g}{{R_h}^2} \quad (42)$$

(ii) the new variables $Z = \bar{R}^3$ and $G = \bar{g}^{1/2}$ are introduced.

(iii) the variable G is used as the independent variable. This has the advantage that the function $Z(G)$ can be found directly from the following equation (no τ dependence):

$$\frac{dZ}{dG} = \frac{6}{\sqrt{\pi}}F_m\frac{1}{\bar{\rho}_g}\left(1 + \int_{g'=0}^{g'=G^2}\frac{\partial\Phi(\bar{R})}{\partial g'}\frac{G}{\sqrt{G^2-g'}}\,dg'\right) \quad (43)$$

and then the corresponding dimensionless time is computed by integrating the following equation:

$$\frac{d\tau}{dG} = \frac{2G}{Z^{4/3}} \quad (44)$$

Assuming the discretization points G_i ($i = 0, 1, 2, 3, \ldots$) and performing a finite analytic integration of the integral in eq 43 with a finite difference approximation of the derivative in it, the following explicit scheme has been developed for the numerical integration of eqs 43 and 44,

$$Z_{i+1} = Z_i + \frac{6F_m}{\sqrt{\pi\bar{\rho}_g}}(G_{i+1} - G_i)\left[1 + 2\sum_{j=1}^{i}\frac{\Phi(\bar{R}_j) - \Phi(\bar{R}_{j-1})}{G_j^2 - G_{j-1}^2}((G_i^2 - G_{j-1}^2)^{1/2} - (G_i^2 - G_j^2)^{1/2})\right] \quad (45)$$

$$\tau_{i+1} = \tau_i + (G_{i+1} - G_i)(G_{i+1} + G_i)\left(\frac{Z_{i+1} + Z_i}{2}\right)^{-4/3} \quad (46)$$

where $Z_o = G_o = \tau_o = 0$. Even with all this pretreatment and careful discretization procedure, a very dense geometrical grid is needed to give accurate results for the bubble radius evolution, particularly at small times.

4. Results−Discussion

The temperature distribution on the surface of the bubble for a bubble size equal to the size of the thermistor ($q = 1$) at several bubble−thermistor distances, h, is shown in Figure 2. It is obvious that the profile converges smoothly as h decreases to a particular shape at $h = 0$ (computationally inaccessible). The profile for $h = 0.01$ used in the present work is practically the same as that for $h = 0.005$ and hopefully as that for $h = 0$.

The temperature distribution on the bubble surface ($h = 0.01$) is shown in Figure 3 for several values of bubble-to-thermistor size ratio. A small bubble ($q = 0.2$) grows inside the thermistor's temperature field, and therefore, it has a temperature close to that of the thermistor. As the bubble grows larger, its surface temperature decreases considerably in regions far away from the thermistor's surface (large θ). These colder regions occupy more and more space as q increases. A comprehensive picture of the entire temperature field can be seen by plotting the isotherms as in Figure 4. Three cases with bubble-to-thermistor radius ratio $q =$ 0.25, 1, and 3 are shown. The difference of the temperature value between two consecutive isotherms is $0.05\times$ $(T_e - T_o)$. It is evident that the existence of the bubble only slightly deforms the temperature field around the thermistor due to the weak (no heat flux) boundary condition on the bubble's surface.

At first, the results of the present theory for the idealized case of no vapor existence (low vapor pressure liquid) and a linear solubility−temperature curve (i.e., $[c_{eq}(T) - c_{eq}(T_o)]/[c_{eq}(T_e) - c_{eq}(T_o)] = (T - T_o)/(T_e - T_o)$ are presented. The great advantage of this case is that the bubble size evolution depends only on the value of the foaming number, F_m, which is actually the measure of the initial driving force for bubble growth. The evolution of the dimensionless bubble size with respect to the dimensional time τ (see eq 42) is shown in Figure 5 for several values of F_m. It must be noted that the results given for relatively small values of F_m ($F_m = 2$) are expected to be poor approximations of the exact ones, since the present theory was derived in the limit of large F_m. As can be seen in the figure, there is an initial short period of fast growth followed by a gradual transition to a larger period which can be characterized as a "linear" growth period. The complete growth curves can be approximated fairly well (except from the early stages) by power law expressions with an exponent value which shows a slight dependence on F_m (i.e., 0.313 for $F_m = 2$; 0.29 for $F_m = 5$; 0.281 for $F_m = 10$; and 0.272 for $F_m = 20$). This behavior contradicts the well-known exponent value 0.5 resulting from the theory of a bubble growing isothermally in an infinite medium. However, the present predictions are in the right direction in the sense that there are experimental results in the literature (not only for dissolved gas bubble growth but also for boiling) described by exponents <0.5.[23]

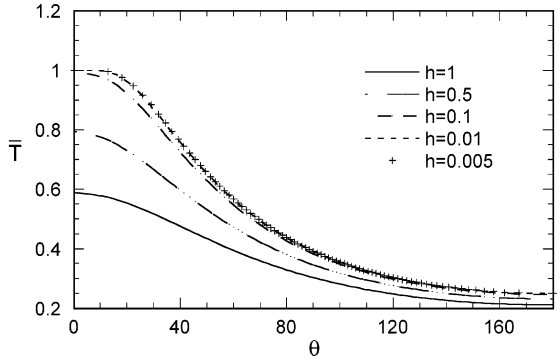

Figure 2. Dimensionless temperature on the surface of the bubble versus angle θ for a bubble-to-thermistor radius ratio $q = 1$ and several values of the bubble−thermistor dimensionless minimum distance h.

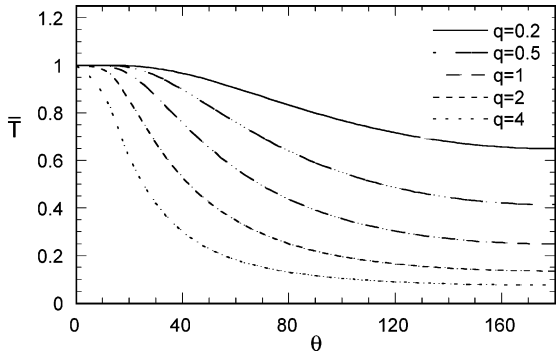

Figure 3. Dimensionless temperature on the surface of the bubble versus angle θ for a bubble−thermistor dimensionless minimum distance $h = 0.01$ and several values of bubble-to-thermistor radius ratio.

To directly assess the effect of the two-dimensionality of the problem on bubble growth behavior, the ratio of the bubble radius from the present theory over the bubble radius for the case of a constant bubble temperature, $T = T_e$, (i.e., $R = 2F_m\sqrt{(3/\pi)t}$ in the fast growth limit) is shown as a function of dimensionless time in Figure 6. Evidently, the bubble radius is much smaller than that in the corresponding constant temperature case. The effect of two-dimensionality (axial symmetry) is a significant reduction of the bubble size (i.e., 10-fold reduction for $F_m = 20$). It is noteworthy that the major part of this reduction occurs at short times corresponding to the initial fast growth period.

A question arising here is what will be the influence of a finite thermal Marangoni number ($Ma_T \neq 0$) on the bubble radius evolution. Fortunately, the answer to this question is straightforward. Marangoni convection transfers hot liquid from the thermistor (bubble base) along the bubble surface, increasing its temperature and, thus, leading to an increase of the driving force for bubble growth. As the Marangoni number increases, the bubble radii ratio in Figure 6 increases, but it can never reach unity because, in the limit $Ma_T = \infty$, an asymptotic temperature profile exists, leading to a growth curve somewhere between the present one corresponding to $Ma_T = 0$ and the constant temperature one. Also,

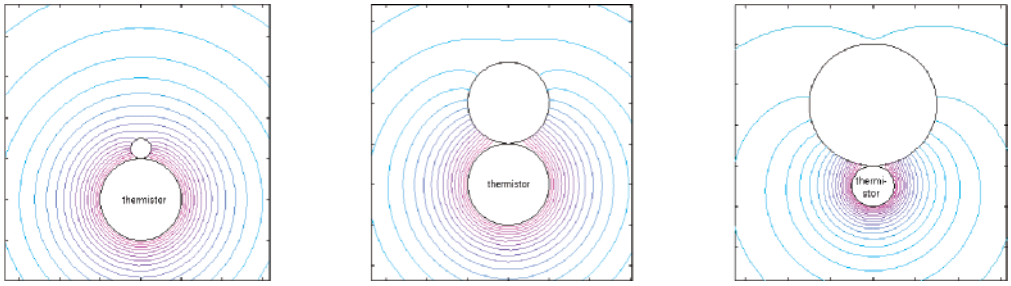

Figure 4. Isotherms (with spacing $0.05(T_e - T_o)$) in the liquid around the bubble−thermistor system for three values of the bubble-to-thermistor radius ratio (q = 0.25, 1, and 3, respectively).

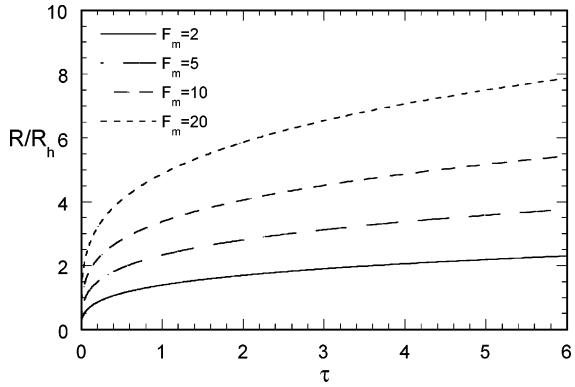

Figure 5. Dimensionless bubble size versus dimensionless time for a linear solubility−temperature dependence curve and several values of the foaming number F_m.

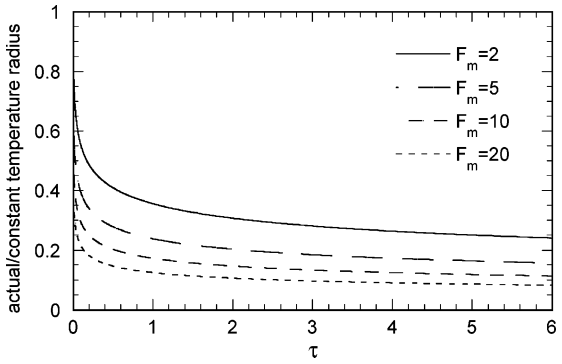

Figure 6. Evolution of the ratio of the radius of a bubble growing on the thermistor (linear solubility−temperature dependence curve) to a radius of a bubble growing at a constant temperature $T = T_e$ for several values of the foaming number F_m.

the power law exponent of the bubble growth curves should increase (as Ma_T increases) from a value ~0.3 (at $Ma_T = 0$) to an asymptotic value (at $Ma_T = \infty$) <0.5. It is important to note that the experimentally determined exponents are ~0.4.[12] An additional complexity arises from the fact that the liquid dragged by Marangoni flow from the thermistor toward the bubble actually originates from the bulk liquid phase (recirculating motion), so it may not have enough time to reach the temperature of the thermistor.

The dimensionless bubble size evolution for the system CO_2−water for an initial bulk water temperature T_o = 20 °C and several values of the thermistor temperature is shown in Figure 7. As the thermistor temperature increases, the bubble grows faster. The shapes of these curves are similar to those of the experimental curves.[12] They consist of a first stage of fast growth (approximated by a power law exponent $^1/_2$ in our previous work) and a second stage of almost linear growth. The corresponding evolution of the vapor

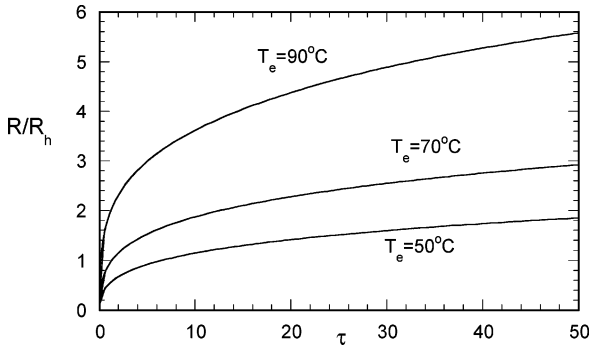

Figure 7. Dimensionless bubble size versus dimensionless time for the system CO_2−water for T_o = 20 °C and several values of the thermistor temperature T_e.

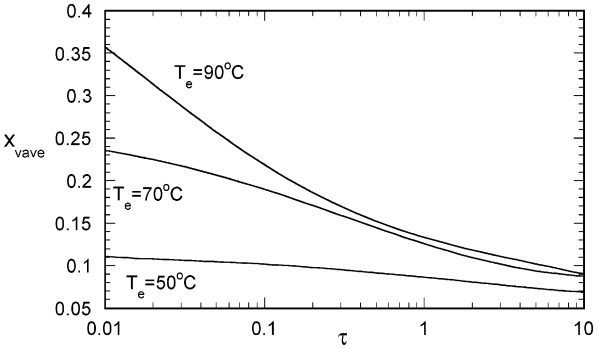

Figure 8. Evolution of total vapor mole fraction in the bubble for the system CO_2−water for T_o = 20 °C and several values of the thermistor temperature T_e.

mole fraction in the bubble is shown in Figure 8. This fraction decreases rapidly during the first stages of growth followed by a smooth decrease at later stages. It must be stressed that, in the above computation, the gas-in-liquid diffusion coefficient is assumed constant, although for the particular gas−liquid system its value increases about 3 times from 20 °C to 90 °C. This variation may be significant for the bubble growth, especially in the case of a high thermistor temperature. Nevertheless, it can be incorporated to the present approximating theory by assuming a time-dependent average diffusion coefficient corresponding to the instantaneous average bubble temperature (based on the thin concentration boundary layer assumption).

The method presented here for the computation of the bubble radius evolution can be also extended for the case of a finite Ma_T. The problem of thermocapillary convection should be solved in a quasi-steady-state formulation for several bubble sizes. The resulting temperature profiles on the surface of the bubble can be used by the present algorithm to find the bubble radius evolution.

It is noted that, in the limit of the thin concentration boundary layer examined here (fast growth with respect

to mass transfer, $F_m \gg 1$) the approximate solution is very important, because any attempt for the solution of the complete problem using multiphase computational fluid dynamics techniques (i.e., volume-of-fluid method) will fail because of the steepness of the concentration profiles and the extremely fast bubble growth dynamics during the first stage of "explosive" growth behavior. Such dynamics can be treated using a combination of Lagrangian coordinate transformation and advanced time-stepping techniques in spherically symmetric problems,[24] but it cannot be handled for the case of complex two-dimensional problems.

5. Conclusions

An approximate solution for a gas bubble growing in contact with a spherical heating element in a liquid is derived here. The approach refers to the case of a thin concentration boundary layer (large foaming number F_m) for which the accurate numerical solution using multiphase computational fluid dynamics codes is extremely difficult. By using the approximate solution, it was found that the bubble grows on the surface of the thermistor according to a power law dependence on time, having an exponent <0.5 (that being the case for a bubble growing isothermally in an infinite medium). This result confirms that the experimental exponents <0.5 found in the literature are inherent to the axial symmetric (two-dimensional) nature of the problem.

Literature Cited

(1) Arefmanesh, A.; Advani, S. G.; Michaelides, E. E. A numerical study of bubble growth during low-pressure foam molding process. *Polym. Eng. Sci.* **1990**, *30*, 1330.

(2) Yoo, H. J.; Han, C. D. Oscillatory behavior of a gas bubble growing (or collapsing) in viscoelastic liquids. *AIChE J.* **1982**, *28*, 1002.

(3) Kislyakov, Y. Y.; Kopyltsov, A. V. The rate of gas-bubble growth in tissue under decompression. Mathematical modeling. *Respir. Physiol.* **1988**, *71*, 299.

(4) Van Liew, H. D.; Burkard, M. E. Simulation of gas bubbles in hypobaric decompressions: Roles of O_2, CO_2, and H_2O. *Aviat., Space Environ. Med.* **1995**, *66*, 50.

(5) Srinivasan, R. S.; Gerth, W. A.; Powell, M. R. A mathematical model of diffusion-limited gas bubble dynamics in tissue with varying diffusion region thickness. *Respir. Physiol.* **2000**, *123*, 153.

(6) Prousevitch, A. A.; Sahagian, D. C.; Anderson, A. J. Dynamics of diffusive bubble growth in magmas. *J. Geophys. Res.* **1983**, *98*, 22283.

(7) Blower, J. D.; Mader, H. M.; Wilson, S. D. R. Coupling of viscous and diffusive controls on bubble growth during explosive volcanic eruptions. *Earth Planet. Sci. Lett.* **2001**, *193*, 47.

(8) Barker, G. S.; Jefferson, B.; Judd, S. J. The control of bubble size in carbonated beverages. *Chem. Eng. Sci.* **2002**, *57*, 565.

(9) Edzwald J. K.; Principles and applications of dissolved air flotation. *Water Sci. Technol.* **1995**, *31*, 1.

(10) Dupre, V.; Ponasse, M.; Aurelle, Y.; Secq, A. Bubble formation by water release in nozzles. I. Mechanisms. *Water Res.* **1998**, *32*, 2491.

(11) Robinson, A. J.; Judd, R. L. Bubble growth in a uniform and spatially distributed temperature field. *Int. J. Heat Mass Transfer* **2001**, *44*, 2699.

(12) Divinis, N.; Panoutsos, C. S.; Michels, A. C.; Sneep, M. C.; de Bruijn, R.; Lotz, H. Th.; Karapantsios, T. D.; Kostoglou, M.; Bontozoglou, V. Bubbles growing in supersaturated solutions at reduced gravity. *AIChE J.* **2004**, *50*, 2369.

(13) Lastochkin, D.; Favelukis, M. Bubble growth in variable diffusion coefficient liquid. *Chem. Eng. J.* **1998**, *69*, 21.

(14) Cable, M.; Frade, J. R. Diffusion-controlled mass transfer to or from spheres with concentration-dependent diffusivity. *Chem. Eng. Sci.* **1987**, *42*, 2525.

(15) Li, Z. M.; Peng, X. F.; Lee, D. J.; Liu, T. Mass transfer behavior at bubble surface during nucleate boiling. *Heat Mass Transfer* **2001**, *38*, 433.

(16) Li, Z. M.; Peng, X. F.; Lee, D. J. Interfacial mass transfer around a vapor bubble during nucleate boiling. *Heat Mass Transfer* **2004**, *41*, 5.

(17) Moon, P.; Spencer, D. E. *Field theory for engineers*; Van Nostrand Company: New York, 1961.

(18) Subramanian, R. S.; Balasubramaniam, R. *The motion of bubbles and drops in reduced gravity*; Cambridge University Press: New York, 2001.

(19) Buehl, W. M.; Westwater, J. W. Bubble growth by dissolution: Influence of contact angle. *AIChE J.* **1966**, *12*, 1.

(20) Plesset, M. S.; Zwick, S. A. The growth of vapor bubbles in superheated liquids. *J. Appl. Phys.* **1954**, *25*, 493.

(21) Ozisik, M. N. *Boundary values problem of heat conduction*; Dover: New York, 1989.

(22) Press, W.; Flannery, B.; Teukolski, S.; Vetterling, W. Numerical Recipes. In *The art of scientific computing*, 1st ed.; Cambridge University Press: New York, 1986.

(23) Strenge, P. H.; Orell, A.; Westwater, J. W. Microscopic study of bubble growth during nucleate boiling. *AIChE J.* **1961**, *7*, 578.

(24) Arefmanesh, A.; Advani, S. G.; Michaelides, E. E. An accurate numerical solution for mass diffusion induced bubble growth in viscous liquids containing limited dissolved gas. *Int. J. Heat Mass Transfer* **1992**, *35*, 1711−1722.

Received for review May 20, 2005
Revised manuscript received July 26, 2005
Accepted August 8, 2005

IE050600C